eXPRESS Polymer Letters Vol.3, No.2 (2009) 84–96
Available online at www.expresspolymlett.com
DOI: 10.3144/expresspolymlett.2009.12

Theoretical and experimental study of foaming process with chain extended recycled PET

I. Coccorullo, L. Di Maio, S. Montesano, L. Incarnato*

Department of Chemical and Food Engineering, University of Salerno, via Ponte don Melillo, I-84084 Fisciano (Salerno), Italy

Received 31 October 2008; accepted in revised form 30 December 2008

Abstract. The theoretical and experimental study of a thermoplastic polymer foaming process is presented. Industrial scraps of PET were used for the production of foamed sheets. The process was performed by making use of a chemical blowing agent (CBA) in the extrusion process. Due to the low intrinsic viscosity of the recycled PET, a chain extender was also used in order to increase the molecular weight of the polymer matrix. Pyromellitic dianhydride (PMDA) and Hydrocerol CT 534 were chosen as chain extender and CBA, respectively. The reactive extrusion and foaming were performed in a two step process.
Rheological characterization was carried out on PET samples previously treated with PMDA, as well as the morphological study was performed to define the cellular structure of the foams produced. Moreover, in order to predict the morphology of the foam, a non isothermal model was developed by taking into account both mass transfer phenomenon and viscous forces effect. Model results were compared with experimental data obtained analyzing the foamed samples. The model was validated in relation to working conditions, chemical blowing agent percentage and initial rheological properties of recycled polymer. A pretty good agreement between experimental and calculated data was achieved.

Keywords: *processing technologies, modeling and simulations, recycling, industrial applications*

1. Introduction

Since their origin in the 1930s, cellular plastics or polymeric foams have received wide success in industrial and consumer applications due to the low material costs, high strength-to-weight ratios, wide range of properties, and ease of processing. Moreover, these materials are particularly attractive since they can be produced with average cell sizes ranging from few microns to hundreds of microns. For any given polymer, the use of different blowing agents and process conditions can yield 'new materials' with different densities, structures, and properties.

Foaming consists of generating tiny gas bubbles in the polymer melt phase in order to produce lightweight materials without sacrificing mechanical and physical properties of the polymer. Gas bubbles can be generated by means of physical or chemical blowing agents. The final foam products usually possess better insulation properties, as well as higher degrees of impact resistance with respect to the starting material, thanks to the presence of the gas bubbles in the polymer melt [1].

There are many types of polymer foaming processes, such as foam extrusion, foam injection molding, compression molding, and micro-foaming [2, 3]. The final foam density depends on the original gas loading, the gas losses to the environment, and the foam expansion at quenching. The cell size and the cell size distribution depend on the intensity and kinetics of nucleation, on the characteristics of the bubble growth processes following

*Corresponding author, e-mail: icoccorullo@unisa.it

nucleation, and on the degree of cell wall collapsing, or cell coalescence, during expansion. Since the performance of foamed polymer is strongly related to many aspects of bubble growth, it is crucial to understand and control the bubble growth during the melt processing [1].

In the last few years the production of poly(ethylene terephthalate) (PET) foamed items, particularly sheets for insulating applications, is encountering a rising interest. Moreover, by the contrast to the commonly used thermoplastic resins, attention was paid to recycled materials [4, 5]. In order to increase the polymer viscosity and to enhance the foamability of recycled PET, various techniques have been investigated, including chain extension by reactive extrusion [4–10].

The results obtained with this technique are encouraging since it allows to perform in a single step the rheological upgrading of recycled polymer and foaming process.

However, in recent years the quality control requirements for plastic foamed products have become increasingly stringent. Therefore, researchers have attempted to optimize the foaming processes in order to produce high quality final products.

One of the most used methods for the optimization of the manufacturing process, as well as final product quality is numerical modeling: a large number of mathematical models for bubble growth were presented in the literature [11–21].

Some models have been written for bubble growth assumed to be governed by mass transfer alone, while others assumed momentum transfer alone. Using an integral method, the combination of these phenomena was presented by some authors. Extensive reviews and references can be found in a monograph edited by Lee and Ramesh [22].

The goal of this work is twofold:

– starting from preliminary results obtained in a previous work [7], the first goal of this work is to improve the process of extrusion foaming by chemical blowing agent (CBA) in order to produce high density foams from PET industrial scraps with a very low viscosity;
– the second goal of this work is to develop a simple and useful tool which can help the companies in choosing foaming conditions without performing complicated laboratory tests. With this aim, according to literature indications [11, 14, 16], the growth of a spherical bubble in a polymeric liquid has been theoretically studied by taking into account both mass transfer phenomenon and viscous forces effect. Moreover, with the aim of predicting the morphology of the final foam, a non isothermal model was developed. Model results were compared with experimental data obtained analyzing foamed sheets produced in laboratory starting from industrial scraps of PET and using a chemical blowing agent. The model was validated in relation to working conditions, chemical blowing agent percentage and initial rheological properties of recycled polymer.

2. Experimental

2.1. Materials

PET industrial scraps of low intrinsic viscosity, coming from the fibre production of a national company (Montefibre, Italy) were used. The chain extender used in this work is the Pyromellitic dianhydride (PMDA) purchased by Aldrich. The chemical modification, in the proportion required for the aim of extrusion foaming, is achieved with very low content of PMDA in PET; specifically three levels of PMDA contents were analyzed: 0.25, 0.50 and 0.75 weight% which proved to be the right compromise to tailor the required rheological modification and suitable foaming processability of PET. As far as the foam production is concerned, the choice was directed to a chemical foaming agent based process. In particular Hydrocerol CT 534, kindly supplied by Clariant, was used as a chemical foaming agent and specifically two levels of Hydrocerol contents were analyzed: 0.30 and 0.50 weight%. It was provided in powder form, and it is classified as an endothermic foaming agent, recommended for PET foaming, based on a mixture of both organic and inorganic foaming substances. The gas yielding during the process is reported as non toxic, presumably a blend of N_2, CO_2 and O_2 with a very low level of water.

2.2. Reactive and foaming processes

The reactive processing of PET with the PMDA and the foaming extrusion process were both performed with a Brabender single screw extruder (D = 20 mm, L/D = 20). The operation was accomplished in two steps.

Table 1. Operating conditions for chemical modification and foaming process

Reactive extrusion process	
Extruder temperature (hopper, barrel) [°C]	280, 280
Static mixer temperature [°C]	290
Die temperature [°C]	270
Screw speed [revolution per minute]	40
Foam extrusion process	
Extruder temperature (hopper, barrel) [°C]	270, 280
Die temperature [°C]	280
Extrusion die: slit die [mm^2]	30×1
Screw speed [revolution per minute]	40

The main operative conditions for chemical modification and foaming process are reported in Table 1. The recycled PET was tailored by the chain extension reaction with the PMDA. The modified polymers were then used for the foam production.

2.2.1. Reactive processing

The reactive processing of PET with the PMDA was realized by making use of the mentioned extruder equipped with a static mixer to allow the required residence time for the reaction between PET and PMDA. The temperature profile used for the extrusion process was the following: extruder temperature (2 zones) 280°C; mixer temperature 290°C; die temperature 270°C. In Table 1, the working conditions for reactive process are reported.

Modified PET was characterized in terms of rheological properties (flow curves, melt strength and breaking stretching ratio (BSR)), mechanical properties (tensile and flexural properties) and densities.

Rheological properties

Rheological behavior of the modified PET was carefully analyzed in this work because this parameter strongly affects the foam morphology.

The dynamic flow properties of the polymer matrix produced by the chain extension process were measured with a Rheometrics Dynamic Spectrometer Mod. RDS-II (Rheometrics, Inc.) using a parallel plates geometry (plate radius = 25 mm; gap = 2 mm). Frequency sweep tests ($\omega = 0.1 \div 100$ rad/s were made at 280°C at a constant strain amplitude (10% strain) under a nitrogen gas purge in order to minimize thermo-oxidative degradation phenomena.

Rheological measurement in shear flow were performed using a Capillary Extrusion Rheometer (Bohlin Instruments) with a die radius of 1 mm and a 16:1 length/diameter, equipped with a twin bore for the Bagley correction. Viscosity measurements were performed at 280°C within a shear rate range of $20 \div 10\,000$ s^{-1}. As the shear rate at the wall is greater for pseudoplastic than for Newtonian fluids at a given volumetric flow rate, the Rabinowitsch corrections were applied in all cases. The Capillary Extrusion Rheometer is equipped with a tensile module. The measurements were performed using a 1 mm diameter capillary die ($L/D = 20$) with the tensile module situated about 20 cm from the extrusion die. An extrusion temperature of 280°C and a wall shear rate of 125 s^{-1} were used. The tests allowed the determination of the melt strength and the breaking stretching ratio (BSR). The samples for testing were dried at 120°C in a vacuum oven for 12 h.

Mechanical properties and densities

The tensile properties were analyzed according to the standard ASTM D-638, the flexural ones were analyzed according to the standard ASTM D-790 and the densities were measured according to the standard ASTM D-1622.

2.2.2. Foaming process

The second step of processing consisted in the foam production by extruding the modified PET with the chemical blowing agent (CBA). Dry blends of treated PET and CBA powder were fed to the previously described extruder apparatus, which was operated without the static mixer. In Table 1 the working conditions for the processes of polymer foaming are reported. Further details on reactive process and foaming can be found elsewhere [7].

Foam produced was characterized in terms of rheological properties (flow curves, melt strength and BSR), mechanical properties (tensile and flexural properties), densities and finally in terms of cell size and cell size distribution by means of scanning electronic microscopy.

Cell size and cell distribution

Cell size and cell distribution was evaluated by means of electronic scanning microscopy (SEM).

In order to evaluate cell size and cell distribution from the SEM micrographs, a software for image analysis was developed and implemented in Labview (National Instruments). This software locates, counts, and measures objects in a rectangular search area. The software uses a threshold on the pixel intensities to segment the objects from their background. Optional filters give the capability to ignore the objects smaller or larger than given sizes. Other options allow rejecting the objects touching the borders of the search area and ignoring the holes that the segmentation process may create in the objects. The segmented objects are then located and measured. The software can also overlay on the image returned the position of the search area, the centers and bounding boxes of the objects detected.

3. Experimental results

3.1. Characterization of modified PET

Modified PET was characterized in terms of rheological properties (flow curves, melt strength and BSR), mechanical properties (tensile and flexural properties) and densities. In Table 2 main experimental results obtained analyzing modified PET samples were reported.

3.1.1. Rheological properties

Rheological behavior of the modified PET was carefully analyzed in this work because this parameter strongly affects the foam morphology.

A significant increase in viscosity due to the use of PMDA as chain extender in PET scraps (PET) is evident from the flow curves reported in Figure 1. These samples also exhibit a pronounced shear thinning behavior particularly the blend PET+ PMDA 0.75%.

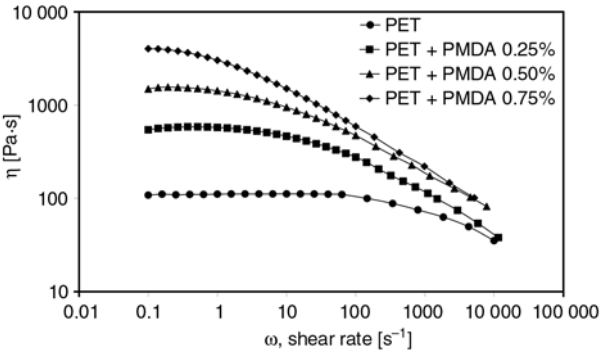

Figure 1. Flow curves for unmodified and modified PET samples (T=280°C)

Values of zero shear viscosity, obtained analyzing rheological data, are reported in Table 2 for unmodified and modified PET samples.

Moreover, in order to verify if the modified PET possesses melt properties suitable for foaming process, melt strength measurements were performed and the results being reported in Table 2. As it can be seen in Table 2, a sharp increase in melt strength is encountered with increasing PMDA content. Both the effects, the shear thinning behaviour and melt strength improvement, can be ascribed to the structural changes occurring during the chain extension process, i.e. the increase in M_w, the broadening of M_w/M_n and branching phenomena accomplished during the reactive extrusion. Actually, too large values of the MS tend to inhibit the bubble growth during the foaming process. As reported later, the parameters so obtained allow in all cases the production of foams, although with some differences. However, the sample treated with 0.50% of PMDA appears as the best accomplishment between the two parameters.

Since the polymer matrix was produced by a chain extension process, we considered the viscosity changing with the chain extender content using a polynomial fittings curve to interpolate the experimental data of η_0 vs. %PMDA [11] using Equation (1):

Table 2. Main properties of the modified PET samples

Code	%PMDA	η_0 [Pa·s] (T=280°C)	Melt strength [10^{-2} N]	BSR	Density [kg/m^3]	η [dl/g]
PET	0	108	not meas.	not meas.	1410	0.49
PET_PMDA025	0.25	543	0.005	80	1414	0.59
PET_PMDA050	0.50	1275	0.012	120	1425	0.67
PET_PMDA075	0.75	3355	0.054	92	1435	0.77

$$\eta_0 (\%PMDA) = 6577 (\%PMDA)^2 - 742.64 (\%PMDA) + 160 \quad (1)$$

Viscosity is related to temperature by an Arrhenius expression [23] and its variation with thermal profile is given by Equation (2):

$$\ln\frac{\eta_{0T}}{\eta_{0T_r}} = \frac{E_a}{R_g}\left(\frac{1}{T} - \frac{1}{T_r}\right) \quad (2)$$

where E_a is an activation energy for viscous flow (94 000 J/mol [23]), η_0 and η_{0T_r} are the zero shear viscosity corresponding to T and T_r, respectively.

The effectiveness of the foaming process is strongly dependent on the viscosity of the polymer matrix and, consequently, on concentration of the chain extender. With an amount of PMDA lower than 0.5% no foam can be obtained.

3.2. Characterization of foam

Foam produced was characterized in terms of rheological properties (flow curves, melt strength and BSR), mechanical properties (tensile and flexural properties), densities and finally in terms of cell size and cell size distribution by means of scanning electronic microscopy. In Table 3 main experimental results obtained analyzing foamed samples were reported.

Data reported in Table 3 show that without significantly sacrifice the mechanical and physical properties (see results of tensile modulus and strength) it is possible to produce lightweight materials.

3.2.1. Cell size and cell distribution

The foamed strips obtained have a closed-cell structure (see SEM micrographs). Closed-cell foams are most suitable for thermal insulation and are produced when the cell membranes are sufficiently strong to withstand rupture at the maximum foam rise.

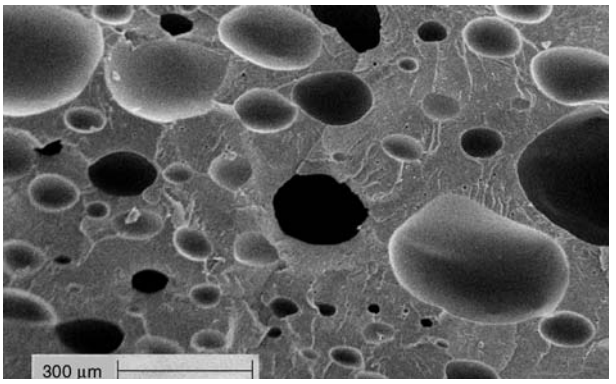

Figure 2. SEM micrograph PET_PMDA050_CBA05

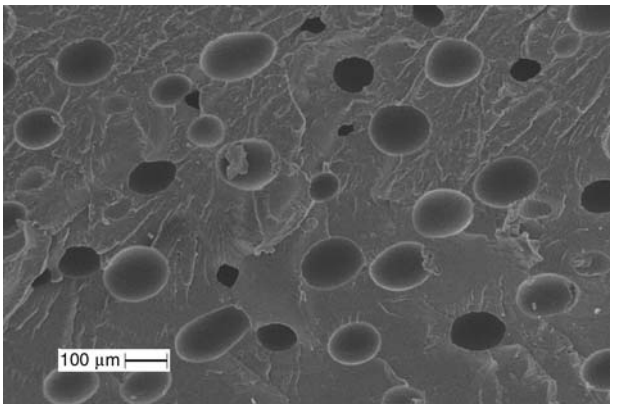

Figure 3. SEM micrograph PET_PMDA075_CBA03

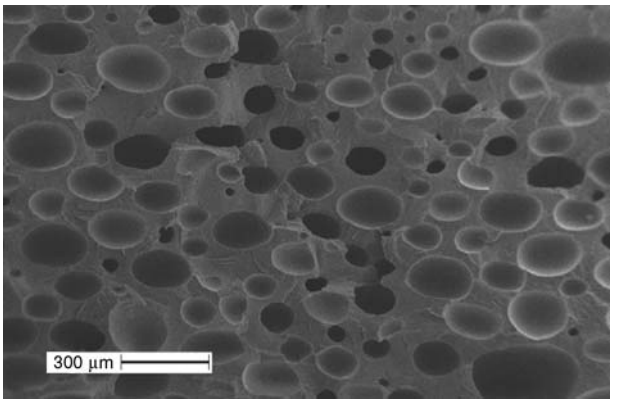

Figure 4. SEM micrograph PET_PMDA075_CBA05

Cell size and cell distribution was evaluated by means of electronic scanning microscopy (SEM). SEM micrographs of the cross section are reported in Figures 2–4 for the samples analyzed in this work.

Table 3. Main properties of the foamed samples

Code	%PMDA	%CBA	Density [kg/m³]	Tensile modulus [MPa]	Tensile strength [MPa]
PET	0	0	1410	1810	55.1
PET_PMDA050_CBA05	0.50	0.50	835	1240	23.4
PET_PMDA075_CBA03	0.75	0.30	1165	1365	29.5
PET_PMDA075_CBA05	0.75	0.50	900	1304	23.8

Table 4. The cell size and cell distribution for samples analyzed in this work

Samples	N bubble [N/mm³]	Cell radius [μm]
PET_PMDA050_CBA05	~110	44 ± 15
PET_PMDA075_CBA03	~330	31 ± 10
PET_PMDA075_CBA05	~290	37 ± 15

Bubble dimensions, as evaluated by the image analysis software, are almost constant in the sample, confirming the assumption that temperature is constant along thickness direction.

The cell size and cell distribution, reported in Table 4, are strongly dependent, during the foaming process, on the concentration of the chain extender and, consequently, on the high viscosity of the polymer matrix.

4. Modeling

4.1. Bubble growth dynamics (Theoretical background)

Consider a polymer melt that has a dissolved gas concentration c_0 in equilibrium with the gas at some elevated pressure P_{B0}. With the release of pressure at $t = 0$, the solution becomes supersaturated, and nucleation and bubble growth begin. As the bubble growth proceeds, the pressure inside the bubble and the dissolved gas concentration at the bubble surface decrease. With time, gas diffuses into the bubble and a concentration gradient propagates radially in the polymer melt. A schematic of the bubble growth is shown in Figure 5. The radius and the dissolved gas concentration are denoted by $R(t)$ and $c(r,t)$.

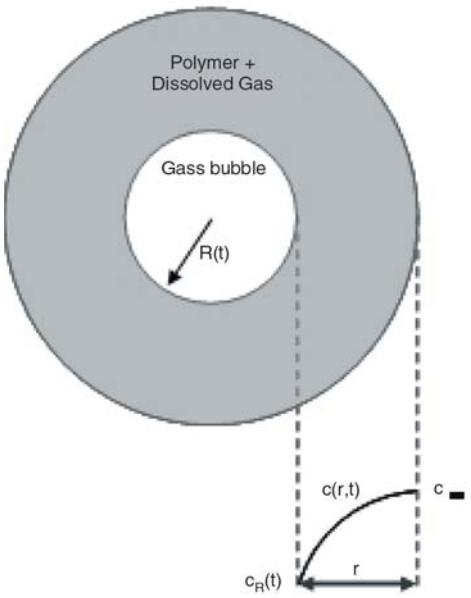

Figure 5. Schematic of single bubble growth

In analyzing the bubbles growth process, the following assumptions can be made:

1. The bubble is spherically symmetric when it nucleates and remains so for the entire period of growth.
2. The gas pressure in the bubble $P_B(t)$ is related to the dissolved gas concentration at the bubble surface $c(R,t)$ by the Henry law: $c(R,t) = K_H P_B(t)$.
3. There are no chemical reactions during bubble growth.
4. Gravitational effects and latent heat of solution are neglected.
5. Inertial effects are neglected and the fluid is assumed to be incompressible and Newtonian.
6. The surface tension at the gas-liquid interface has a constant value σ.
7. The effect of foam densities on thermal conductivity of gas-filled polymeric bubble system is neglected.

The material properties such as polymer structure, molecular weight and its distribution, crystallinity and others are independent of the dissolved gas concentration and are ignored.

The neglect of inertia and the assumption of Newtonian behavior is imposed because the fluids are very viscous and the initial bubble growth rates are very small. Nevertheless, Amon and Denson [13] studied heat transfer analysis in polymer-gas systems in great detail. They found from reliable empirical correlations that the effective thermal conductivity of gas-filled polymeric bubble system changes by no more than a few percentage points over the whole range of foam densities. Moreover, as for thermoplastic foam extrusion, growth occurs in the molten-to-solid transition state. The polymer is cooled from 280°C (die temperature) to 25°C (ambient temperature) in a relatively short time: since in these circumstances all physical properties of the system undergo a rapid change, a transient heat transfer problem is considered here.

4.2. Governing equations for the bubble growth

In view of the above restrictions, the equation of motion, integral mass (gas) balance over the bubble and differential mass (dissolved gas) balance in the

surroundings mother phase take the following forms [14]. Equation of motion is given by Equation (3):

$$\frac{dR}{dt}=\frac{P_B-P_C}{4\eta}R-\frac{\sigma}{2\eta} \tag{3}$$

The initial condition for the above equation is: $R(0) = R_i$. Here R_i is the initial radius of the bubble, P_C the pressure in the continuous phase, σ surface tension and η melt viscosity.

Integral mass (gas) balance over the bubble

A differential mass balance in a binary system assuming spherical symmetry, constant density and diffusion coefficient (D) is of the form of Equation (4):

$$\frac{\partial c}{\partial t}+v_r\frac{\partial c}{\partial r}=D\left[\frac{1}{r^2}\frac{\partial}{\partial r}\left(r^2\frac{\partial}{\partial r}\right)\right] \tag{4}$$

where c is the dissolved gas concentration in the melt and D is the binary diffusion coefficient. The boundary and initial conditions for Equation (4) are given by Equation (5):

$$\begin{aligned} &c(r,0)=c_i(r)\\ &c(R,t)=c_R(t)=K_H P_B(t)\\ &c(\infty,t)=c_\infty \end{aligned} \tag{5}$$

At a distance far from the bubble surface, the solution is not affected by the growing bubble and the dissolved gas concentration remains c_∞, the same as before the onset of nucleation. The quantity c_R is the dissolved gas concentration at the bubble surface. It is related to the gas pressure in the bubble through the solubility coefficient K_H. The quantity $c_i(r)$ is the initial concentration profile in the melt. The mass balance on the bubble requires that the rate of mass added to the bubble equals the rate that mass diffuses in through the bubble surface. Thus, a simple mass balance at the bubble surface relates the bubble pressure to the concentration gradient at the surface (see Equation (6)):

$$\frac{d}{dt}\left(\frac{4\pi}{3}\frac{P_B R^3}{Z_2 R_g T}\right)=4\pi R^2 D\left.\frac{dc}{dr}\right|_{r=R} \tag{6}$$

The initial condition for the above equation is $P_B(0) = P_{B0}$. Here P_{B0} is the initial bubble pressure, Z_2 the compressibility factor of the gas inside the bubble, T temperature and R_g universal gas constant.

4.2.1. Dimensionless form of the governing equations

To facilitate the subsequent analysis, the following dimensionless variables and groups can be defined by Equations (7)–(15):

$$c_a=\frac{c-K_H P_C}{c_\infty-K_H P_C} \tag{7}$$

$$P_{Ba}=\frac{P_B-P_c}{P_{B0}-P_c} \tag{8}$$

$$r_a=\frac{r}{R_C} \tag{9}$$

$$R_a=\frac{R}{R_C} \tag{10}$$

$$t_a=\frac{t}{t_c} \tag{11}$$

$$N_G=\frac{16\pi\sigma^3}{3k_B T(P_{B0}-P_c)^2} \tag{12}$$

$$N_{Pe}=\frac{\sigma^2}{\eta D(P_{B0}-P_c)} \tag{13}$$

$$N_{pi}=\frac{P_C}{P_{B0}-P_c} \tag{14}$$

$$N_{si}=K_H RT \tag{15}$$

In defining the above dimensionless quantities, we picked the critical bubble radius (Equation (16)):

$$R_C=\frac{2\sigma}{P_{B0}-P_C} \tag{16}$$

and the critical momentum transfer time (Equation (17)):

$$t_C=\frac{4\eta}{P_{B0}-P_C}, \tag{17}$$

as our characteristic bubble radius and bubble growth time, respectively.

In terms of the dimensionless variables, the equations governing the bubble growth dynamics takes the following forms (see Equations (18)–(20)):

$$\frac{dR_a}{dt_a} = P_{Ba}R_a - 1 \tag{18}$$

$$\frac{dP_{Ba}}{dt_a} = \frac{3Z_2N_{si}}{N_{Pe}}\frac{1}{R_a}\frac{\partial c_a}{\partial r_a}\bigg|_{r_a=R_a} - \frac{3(P_{Ba}+N_{pi})}{R_a}\frac{dR_a}{dt_a} \tag{19}$$

$$\frac{\partial c_a}{\partial r_a} + \frac{R_a^2}{r_a^2}\frac{dR_a}{dt_a}\frac{\partial c_a}{\partial r_a} = \frac{1}{r_a^2N_{Pe}}\frac{\partial}{\partial r_a}\left(r_a^2\frac{\partial c_a}{\partial r_a}\right) \tag{20}$$

The corresponding initial and boundary conditions are given by Equations (21)–(25):

$$R_a(0) = R_{ai} \tag{21}$$

$$P_{Ba}(0) = PB_{ai} \tag{22}$$

$$c_a(r_a,0) = c_{ai}(r_a) \tag{23}$$

$$c_a(R_a,t_a) = P_{Ba} \tag{24}$$

$$c_a(\infty,t_a) = 1 \tag{25}$$

Since the critical cluster represents an equilibrium state, this specification of the initial conditions will not produce bubble growth. To achieve the latter, we must perturb one or more of these variables from the equilibrium state. The bubble growth is a strong function of the value of the initial radius, arbitrary choice of it can lead to considerable error [11].

4.2.2. Initial conditions for bubble growth

In order to calculate the initial conditions for bubble growth, the approach used follows from Shafi *et al*. [11]. Following this procedure, we get the initial conditions for bubble growth (see Equations (26) and (27)):

$$R_a(0) = (1+A) + \frac{A(1+A)^2N_{Pe}}{3N_{si}} \tag{26}$$

$$P_B(0) = 1 - \frac{A(1+A)(1+N_{pi})N_{Pe}}{N_{si}} \tag{27}$$

where A is defined by Equation (28):

$$A = \left[1 + \left(\frac{3\pi}{4N_G}\right)^{\frac{1}{2}}\right]^{\frac{1}{3}} - 1 \tag{28}$$

The methodology for handling the transport processes around a single expanding bubble is valid for a bubble growing in an infinite expanse of liquid with no dissolved gas limitations. In actual foaming, there is a finite amount of dissolved gas that is continuously depleted by the simultaneous growth and nucleation of bubbles.

In order to extend the analysis in a finite amount of dissolved gas, in this work, the procedure presented by Shafi *et al*. [11] was adopted (see Figure 5). Shafi *et al*. applying the integral method to the present problem introduce an undetermined function of time, V_{cb}. Physically it represents the volume of the melt between the bubble surface and the radial position where the dissolved gas concentration approaches the initial dissolved gas concentration c_0. Moreover, they define two new variables: x, which represents the melt volume between the bubble surface and radial position r normalized to the volume of concentration boundary region V_{cb} and also a new concentration variable C as in Equations (29) and (30):

$$x = \frac{4\pi}{3}\frac{r^3 - R^3}{V_{cb}} \tag{29}$$

$$C = \frac{c - c_R}{c_0 - c_R} \tag{30}$$

Equations (29) and (30) transform a moving boundary problem with variable boundary conditions to a fixed boundary problem with constant boundary conditions. C is always 0 at the bubble surface ($x = 0$), and is 1 at the far end of the concentration boundary ($x = 1$) and it can be assumed as a function of x only. In view of Equations (29) and (30) and defining additional dimensionless variables and groups as shown in Equations (31) and (32):

$$c_{Ra} = \frac{c_R - K_HP_B}{c_0 - K_HP_B} \tag{31}$$

$$V_{cba}=\frac{3V_{cb}}{4\pi R_c^3} \tag{32}$$

the equations governing the bubble growth dynamics in terms of dimensionless quantities can be rewritten by Equations (33)–(35):

$$\frac{\mathrm{d}R_a}{\mathrm{d}t_a}=c_{Ra}R_a-1 \tag{33}$$

$$\frac{\mathrm{d}c_{Ra}}{\mathrm{d}t_a}=\frac{9N_{si}Z_2}{N_{Pe}}\frac{(1-c_{Ra})R_a}{V_{cba}}\frac{\mathrm{d}c}{\mathrm{d}x}\bigg|_{x=0}-\frac{3(c_{Ra}+N_{pi})}{R_a}\frac{\mathrm{d}R_a}{\mathrm{d}t_a} \tag{34}$$

$$V_{cba}=\frac{(c_{Ra}+N_{pi})R_a^3-(1+N_{pi})}{N_{si}(1-c_{Ra})\int_0^1(1-C)\mathrm{d}x} \tag{35}$$

With the initial conditions given by Equations (36) and (37):

$$R_a(0)=(1+A)+\frac{A(1+A)^2N_{Pe}}{3N_{si}} \tag{36}$$

$$c_R(0)=1-\frac{A(A+1)(1+N_{pi})N_{Pe}}{N_{si}} \tag{37}$$

4.3. Model formulation

In order to calculate the evolution of the bubbles size in the foam sheet starting from material properties and working conditions, the model above described was implemented in a simulation code developed in Labview (National Instruments). With this aim Equations (33)–(35) must be solved with the initial conditions given by Equations (36) and (37). Moreover, as for thermoplastic foam extrusion, growth occurs in the molten-to-solid transition state. The polymer is cooled from 280°C (die temperature) to 25°C (ambient temperature). Rheological property variation certainly changes the isothermal growth scenario and hence, a transient heat transfer problem is considered here. The polymer is cooled by means of two cooling fans, in this case, the energy equation combined with Fourier's law of heat conduction, is given by Equation (38):

$$\frac{\partial T}{\partial t}=\frac{k_P}{\rho_P C_{p,P}}\frac{\partial^2 T}{\partial x^2} \tag{38}$$

where ρ_P, $C_{p,P}$ and k_p are density, specific heat and thermal conductivity, respectively.
The initial and boundary conditions are then given by Equation (39):

$$\begin{aligned} &T=T_0,\ t=t_0\\ &\frac{\partial T}{\partial x}=0,\ x=0\\ &\frac{\partial T}{\partial x}=h(T-T_{AIR}),\ x=\delta \end{aligned} \tag{39}$$

where δ is the half-thickness of the foam sheet, T_0 is the initial temperature of the polymer (die temperature), T_{AIR} is the ambient temperature and h is the heat transfer coefficient.

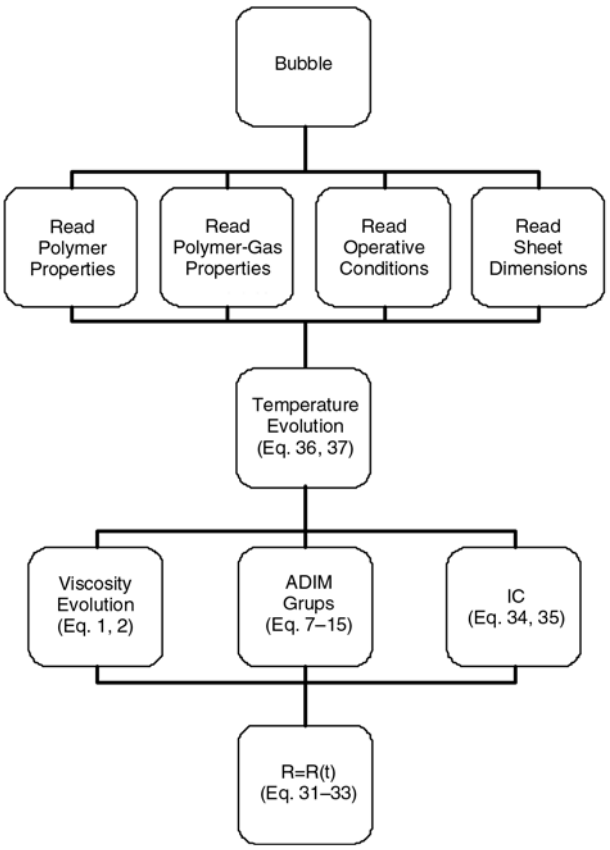

Figure 6. Flow chart describing the sequence of the calculations in the model

A flow chart describing the sequence of the calculations is reported in Figure 6. In Table 5, the main variables involved in the model are reported.

4.3.1. Solution methodology

The equations governing the bubble growth dynamics are highly nonlinear and stiff. These equations were solved using the Gear's method. The nonlinear equations are solved by Brown's method. The equations were solved using a finite difference scheme.

It is worth mentioning that in the model adopted in this work there are no involved adjustable parameters so that the model starting from data of materials properties and the operative conditions is able to predict bubble dimensions.

5. Model results

Model developed in this work following the literature indications allows to calculate the evolution of the temperature, of the bubble pressure and radius starting from the operative conditions and material properties (Tables 1 and 6). Consistently with experimental data, with an amount of chain extender lower that 0.5% according to the model the clusters are not sufficiently large compared to the critical cluster in order to grow spontaneously to a macroscopic bubble and no foam can be obtained. In Figure 7, the calculated evolution of temperature and bubble radius during the foaming process are reported for PET_PMDA050_CBA05 and PET_PMDA075_CBA05. Figures show that bubbles growth takes about one second, after this time temperature become too low and viscosity too high.

Table 5. Main variables involved in the model adopted in this work

σ	surface tension	D	binary diffusion coefficient
η	melt viscosity	Z_2	compressibility factor of the gas
K_H	solubility coefficient	R_g	Universal gas constant
P_{B0}	initial bubble pressure	c_∞	initial gas concentration
R_i	initial radius of the bubble	$c_i(r)$	initial gas concentration profile
$R(t)$	bubble radius	$c(r,t)$	dissolved gas concentration
$P_B(t)$	gas pressure in the bubble	$c(R,t)=c_R$	dissolved gas concentration at the bubble surface
P_C	Pressure in the continuous phase		
V_{cb}	volume of the melt between the bubble surface and the radial position where the dissolved gas concentration approaches the initial dissolved gas concentration c_0		

Table 6. Physical properties [23] and operative conditions used in the model

Physical properties	Operative conditions
PET specific heat C_p	1130 J/(kg·K)
Thermal conductivity K	0.218 W/(m·K)
Activation energy for viscous flow E_a	94 000 J/mol
Rheological reference temperature	553 K
Surface tension σ	0.0446 N/m
Diffusivity	$3\cdot10^{-12}$ m^2/s
Die pressure	$1.5\cdot10^6$ Pa
Ambient pressure	$1.01\cdot10^5$ Pa
Die temperature T_0	543 K

In Figure 8, the calculated evolution of bubble pressure and radius during the foaming process are reported for PET_PMDA050_CBA05 and PET_PMDA075_CBA05.

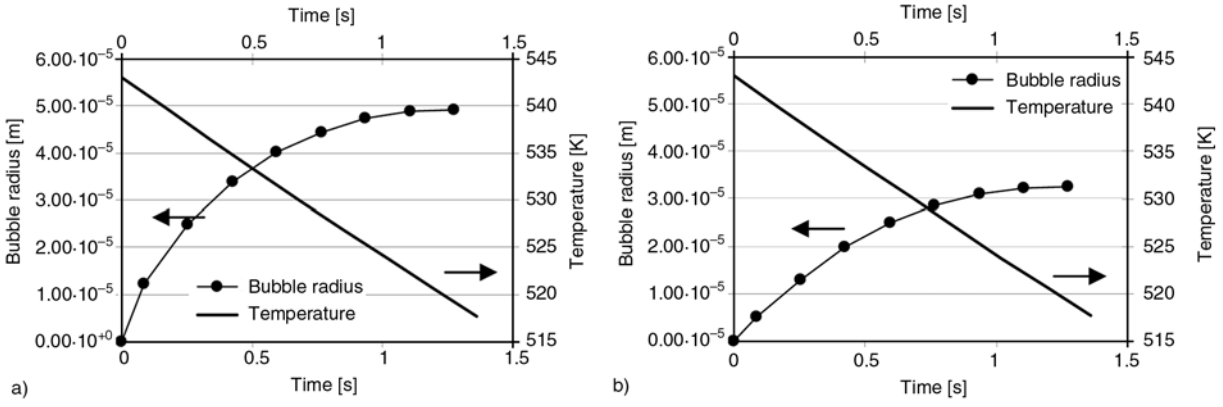

Figure 7. Temperature profile for the bubble growth simulation of extrusion. a – PET_PMDA050_CBA05; b – PET_PMDA075_CBA05

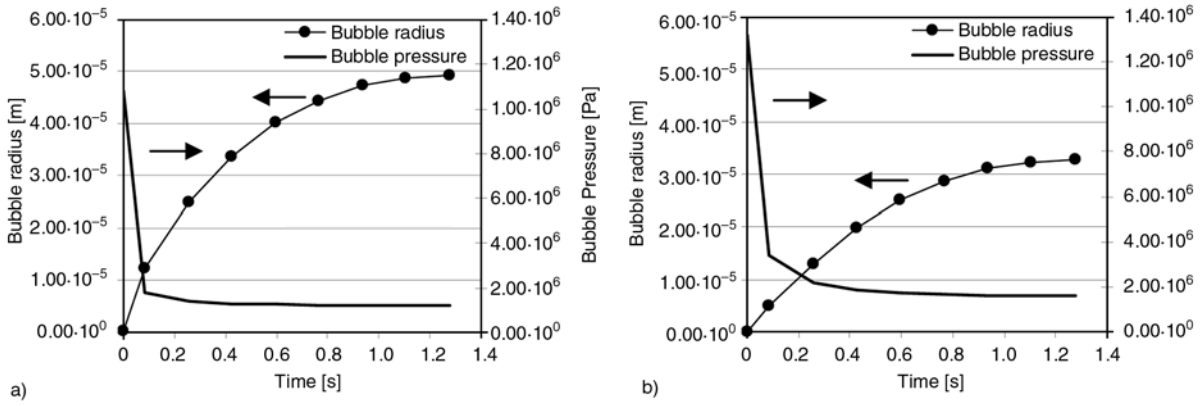

Figure 8. Pressure profile for the bubble growth simulation of extrusion foaming, a – PET_PMDA050_CBA05; b – PET_PMDA075_CBA05

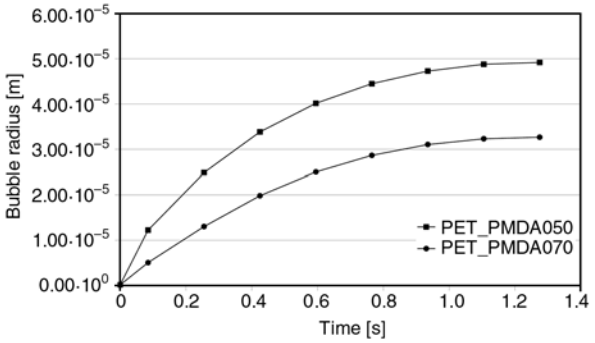

Figure 9. Evolution of the bubble radius for PET_PMDA050_CBA05 and PET_PMDA075_CBA05

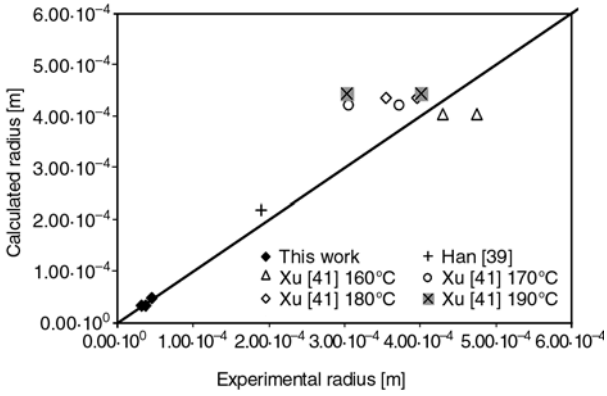

Figure 10. Comparison between experimental results and model prediction for the bubble radius (literature data are also reported in figure)

The bubble pressure start from a maximum and decreases to a value close to the ambient pressure.

The evolution of the bubble radius for the samples analyzed in this work was compared in Figure 9. As it can be seen from the figure, the radius of the bubbles in the sample coded as PET_PMDA050_CBA05 is bigger than the one of the bubbles in PET_PMDA075_CBA05. From figure the effect of the PMDA content is evident, in fact, the bubble radius increases on decreasing of the PMDA content: this is mainly due to the higher melt strength (shown by the PET_PMDA075_CBA05) which limits the growth of the bubbles.

The comparison between experimental results and model prediction for the bubble radius is reported in Figure 10. Because at the moment only few experimental data are available, literature data [25, 26] are also reported in figure. Moreover, the model described in this work was adopted in order to calculate the evolution of the bubble radius in literature experimental conditions and results were also reported in figure. The satisfactorily agreement between literature experimental data and model predictions is a further validation of the model adopted in this work.

Table 7. Comparison between experimental results and model prediction for the bubble radius

Samples	Experimental cell radius [μm]	Calculated cell radius [μm]
PET_PMDA050_CBA05	44 ± 15	49
PET_PMDA075_CBA03	31 ± 10	33
PET_PMDA075_CBA05	37 ± 15	33

In order to underline results achieved in this work, the comparison between experimental results and model prediction for the bubble radius for PET_PMDA050_CBA05, PET_PMDA075_CBA03, PET_PMDA075_CBA05 is reported in Table 7. Comparison shows that model seems to be able to predict experimental data of bubble radius, even if, at the moment only few experimental data are available.

The comparison between experimental data and model prediction shown in Figure 10 is satisfactorily, however, better results of prediction of the evolution of the bubble radius during foaming process could be achieved by means of a better rheological description, that is adopting more complex models which better describe viscoelastic properties of the material.

5. Conclusions

In this work, the process of extrusion foaming by chemical blowing agent (CBA) was improved in order to produce high density foams from PET industrial scraps with a very low viscosity. Due to the low intrinsic viscosity of the recycled PET (IV = 0.48 dl/g), a chain extender was also used in order to increase the molecular weight of the polymer matrix. The reactive processing of PET and the foaming extrusion process were both performed with a Brabender single screw extruder. The operation was accomplished in two steps. The chemical modification, in the proportion required for the aim of extrusion foaming, is achieved with very low content of PMDA in PET; specifically three levels of PMDA contents were analyzed: 0.25, 0.50 and 0.75 weight% which resulted to be the right compromise to tailor the required rheological modification and suitable foaming processability of PET. As far as the foam production is concerned, the choice was directed to a chemical foaming agent based process. In particular Hydrocerol CT 534 was used as a chemical foaming agent and specifically two levels of Hydrocerol contents were analyzed: 0.30 and 0.50 weight%.

Modified PET was characterized in terms of rheological properties (flow curves, melt strength and BSR), mechanical properties (tensile and flexural properties) and densities. Foam produced was characterized in terms of rheological properties (flow curves, melt strength and BSR), mechanical properties (tensile and flexural properties), densities and finally in terms of cell size and cell size distribution by means of scanning electronic microscopy.

Finally, the growth of a spherical bubble in a polymeric liquid has been theoretically studied by taking into account both mass transfer phenomenon and viscous forces effect.

Model results were compared with experimental data obtained analyzing foamed sheets produced in laboratory starting from industrial scraps of PET. As for thermoplastic foam extrusion, growth occurs in the molten-to-solid transition state. Rheological property variation certainly changes the isothermal growth scenario and hence, a transient heat transfer problem is considered and a non isothermal model for bubble growth was developed.

The model was validated in relation to working conditions, chemical blowing agent percentage and initial rheological properties of recycled polymer. A good agreement between experimental and calculated data was achieved, even if, at the moment only preliminary experimental data are available.

In order to achieve a better understanding of the foaming process, future work will consider an additional validation by comparing model results with a wider set of experimental data and the analysis of the bubble nucleation.

References

[1] Lee C. H., Lee K-J., Jeong H. G., Kim S. W.: Growth of gas bubbles in the foam extrusion process. Advances in Polymer Technology, **19**, 97–112 (2000). DOI: 10.1002/(SICI)1098-2329(200022)19:2<97::AID-ADV3>3.0.CO;2-B

[2] Kumar V., Suh N. P.: Process for making microcellular thermoplastic parts. Polymer Engineering and Science, **30**, 1323–1329 (1990). DOI: 10.1002/pen.760302010

[3] Baldwin D. F., Suh N. P., Park C. B., Cha S. W.: Supermicrocellular foamed materials, U.S. Patent 5334356, USA (1994).

[4] Xanthos M., Dey S.: Foam extrusion of polyethylene terephthalate (PET). in 'Foam extrusion: Principles and practice' (ed.: Lee S. T.) Technomic, Lancaster, 307–336 (2000).

[5] Branch G. L., Wardle T.: Manufacture of fully recyclable foamed polymer from recycled material. International Patent PCT/US2004/015245 (2004).

[6] Incarnato L., Scarfato P., Di Maio L., Acierno D.: Structure and rheology of recycled PET modified by reactive extrusion. Polymer, **41**, 6825–6831 (2000). DOI: 10.1016/S0032-3861(00)00032-X

[7] Di Maio L., Coccorullo I., Montesano S., Incarnato L.: Chain extension and foaming of recycled PET in extrusion equipment. Macromolecular Symposia, **228**, 185–200 (2005). DOI: 10.1002/masy.200551017

[8] Awaja F., Dumitru P.: Statistical models for optimisation of properties of bottles produced using blends of reactive extruded recycled PET and virgin PET. European Polymer Journal, **41**, 2097–2106 (2005). DOI: 10.1016/j.eurpolymj.2005.04.010

[9] Japon S., Boogh L., Leterrier Y., Manson J. A. E.: Reactive processing of poly(ethylene terephthalate) modified with multifunctional epoxy-based additives. Polymer, **41**, 5809–5818 (2000).
DOI: 10.1016/S0032-3861(99)00768-5

[10] Awaja F., Pavel D.: Injection stretch blow moulding process of reactive extruded recycled PET and virgin PET blends. European Polymer Journal, **41**, 2614–2634 (2005).
DOI: 10.1016/j.eurpolymj.2005.05.036

[11] Shafi M. A., Lee J. G., Flumerfelt R. W.: Prediction of cellular structure in free expansion polymer foam processing. Polymer Engineering and Science, **36**, 1950–1959 (1996).
DOI: 10.1002/pen.10591

[12] Venerus D. C.: Diffusion-induced bubble growth in viscous liquids of finite and infinite extent. Polymer Engineering and Science, **41**, 1390–1398 (2001).
DOI: 10.1002/pen.10839

[13] Amon M., Denson C. D.: A study of the dynamics of foam growth: Analysis of the growth of closely spaced spherical bubbles. Polymer Engineering and Science, **24**, 1026–1034 (1984).
DOI: 10.1002/pen.760241306

[14] Favelukis M., Zhang Z., Pai V.: On the growth of a non-ideal gas bubble in a solvent-polymer solution. Polymer Engineering and Science, **40**, 1350–1359 (2000).
DOI: 10.1002/pen.11264

[15] Ramesh N. S., Rasmussen D. H., Campbell G. A.: The heterogeneous nucleation of microcellular foams assisted by the survival of microvoids in polymers containing low glass transition particles. Part I: Mathematical modeling and numerical simulation. Polymer Engineering and Science, **34**, 1685–1697 (1994).
DOI: 10.1002/pen.760342206

[16] Patel R. D.: Bubble growth in a viscous Newtonian liquid. Chemical Engineering Science, **35**, 2352–2356 (1980).

[17] Joshi K., Lee J. G., Shafi M. A., Flumerfelt R. W.: Prediction of cellular structure in free expansion of viscoelastic media. Journal of Applied Polymer Science, **67**, 1353–1368 (1998).
DOI: 10.1002/(SICI)1097-4628(19980222)67:8<1353::AID-APP2>3.0.CO;2-D

[18] Yue P., Feng J. J., Bertelo C. A., Hu H. H.: An arbitrary Lagrangian-Eulerian method for simulating bubble growth in polymer foaming. Journal of Computational Physics, **226**, 2229–2249 (2007).
DOI: 10.1016/j.jcp.2007.07.007

[19] Otsuki Y., Kanai T.: Numerical simulation of bubble growth in viscoelastic fluid with diffusion of dissolved foaming agent. Polymer Engineering and Science, **45**, 1277–1287, (2005).
DOI: 10.1002/pen.20395

[20] Everitt S. L., Harlen O. G., Wilson H. J.: Competition and interaction of polydisperse bubbles in polymer foams. Journal of Non-Newtonian Fluid Mechanics, **137**, 60–71 (2006).
DOI: 10.1016/j.jnnfm.2006.03.005

[21] Favelukis M.: Dynamics of foam growth: Bubble growth in a limited amount of liquid. Polymer Engineering and Science, **44**, 1900–1906 (2004).
DOI: 10.1002/pen.20192

[22] Lee J. G., Ramesh N. S.: Polymeric foams: Mechanisms and materials. CRC Press, New York (2004).

[23] Van Krevelen D. W.: Properties of polymers. Elsevier, New York (1990).

[24] Amon M., Denson C. D.: A study of the dynamics of foam growth: Simplified analysis and experimental results for bulk density in structural foam molding. Polymer Engineering and Science, **26**, 255–267 (1986).
DOI: 10.1002/pen.760260311

[25] Han C. D., Yoo H. J.: Studies on structural foam processing. 4. Bubble growth during mold filling. Polymer Engineering and Science, **21**, 518–533 (1981).

[26] Xu D., Pop-Iliev R., Park C. B., Fenton R. G., Jiang H.: Fundamental study of CBA-blown bubble growth and collapse under atmospheric pressure. Journal of Cellular Plastics, **41**, 519–538 (2005).
DOI: 10.1177/0021955X05059031